Supporting Information

Cytotoxicity of *fac*-Mn(CO)$_3$ complexes with a bidentate quinoline ligand towards triple negative breast cancer

Danira A. Habashy,[a] Rabaa M. Khaled,[b] Amr Y. Ahmed,[a] Krzysztof Radacki,[c] Salma K. Ahmed,[d] Engy Khaled,[d] Hana Magdy,[d] Alaa Zeinhom, [d] and Ahmed M. Mansour,*[b]

[a.] *Department of Pharmacology, Toxicology and Clinical Pharmacy, German University in Cairo, New Cairo, Egypt.*
[b.] *Department of Chemistry, Faculty of Science, Cairo University, Gamma Street, Giza, Cairo 12613, Egypt.* E-mail: mansour@sci.cu.edu.eg; inorganic_am@yahoo.com
[c.] I*nstitut für Anorganische Chemie, Julius-Maximilians-Universität Würzburg, Am Hubland, D-97074 Würzburg, Germany.*
[d.] *Department of Biotechnology, Faculty of Science, Cairo University, Gamma Street, Giza, Cairo 12613, Egypt.*

Section A: Experimental

Materials and instruments

Quinoline-2-carboxaldehyde, 8-aminoquinoline, bromo penta-carbonyl manganese(I) and organic solvents were obtained from commercial resources and used as received. Advion compact mass spectrometer was used for recording positive and negative mode electrospray ionization mass spectra. A Specord 210 Plus spectrophotometer was utilized for recording electronic absorption spectra. IR spectra of solid complexes were recorded on a Bruker Alpha-E instrument. ^{1}H NMR analysis was performed using a Bruker Avance 400. The elemental analyses were determined on an automatic CHNS analyzer, Vario EL III Elementar.

Synthesis

To a flat-bottomed flask charged with either 8-aminoquinoline (0.34 mmol; 54 mg) or quinoline-2-carboxaldehyde (0.36 mmol; 110 mg) and bromo penta-carbonyl manganese(I) (0.38 mmol; 105 mg), *n*-hexane (15 mL) was added. Under the dark conditions, the flasks were heated to reflux for 45 minutes. Reddish brown (**A**) and yellow (**B**) precipitates were formed on hot. The products were collected, washed with *n*-hexane, and then dried. **A**: Yield: 76% (92 mg, 0.27 mmol). IR (ATR): *v* = 2021 (vs, C≡O), 1929 (sh, C≡O), 1906 (vs, C≡O), 1593, 1550, 1394, 1249 cm^{-1}. ESI-MS (positive mode, acetone): *m/z* = 298.8 {M–Br}$^{+}$ and 211.9 {M–Br–3CO}$^{+}$ (M = molecular mass). $C_{13}H_7BrMnNO_4{\cdot}2H_2O$: C 37.89, H 2.69, N 3.40 found: C 38.06, H 2.31, N 3.68. **B**: Yield: 74.4% (28.1 mg, 0.26 mmol). IR (ATR): *v* = 2021 (vs, C≡O), 1932 (sh, C≡O), 1899 (vs, C≡O), 1565, 1507, 822 cm^{-1}. ^{1} H NMR (CD_3COCD_3, 400.40 MHz): δ = 9.46 (d, $^{3}J_{H,H}$ = 4.89 Hz, 1H, Q-H2), 8.60 (d, $^{3}J_{H,H}$ = 8.43 Hz, 1H, Q-H4), 8.03 (d, $^{3}J_{H,H}$ = 7.83 Hz, 1H, Q-H5), 7.99 (d, $^{3}J_{H,H}$ = 6.60 Hz, 1H, Q-H7), 7.79 (m, 1H, Q-H3), 7.75 (d, $^{3}J_{H,H}$ = 7.70 Hz, 1H, Q-H6), 7.10 (d, $^{2}J_{H,H}$ = 12.59 Hz, 1H, NH_2), and 5.46 (d, $^{2}J_{H,H}$ = 12.10 Hz, 1H, NH_2) ppm. ESI-MS (positive mode, acetone): *m/z* = 360.8 {M-H}$^{-}$ and 198.8 {M–Br–3CO}$^{+}$. $C_{12}H_8BrMnN_2O_3{\cdot}0.5H_2O$: C 38.82, H 2.42, N 7.54, found: C 39.11, H 2.52, N 7.58.

Single crystal X-ray diffraction analysis

Slow evaporation of solution of **B** in acetone over two weeks offered orange crystals suitable for X-ray crystallographic analysis. The diffraction data of **B** were acquired at 100 K using a RIGAKU XtaLAB Synergy-R diffractometer equipped with a semiconductor HPA-detector (HyPix-6000) and multi-layer mirror mono-chromated *Cu-K$_\alpha$* radiation. The intrinsic phasing approach (SHELXT programme) was used to solve the structure of the manganese tricarbonyl complex (**B**),[1] which was then improved using the SHELXL programme and the SHELXLE graphical user interface.[2] Non-hydrogen atoms were refined using an anisotropic approximation, whereas hydrogen atoms were 'riding' on idealised locations. Crystal data for **B**: $C_{12}H_8BrMnN_2O_3$, M_r = 363.05, orange block, 0.289 × 0.241 × 0.071 mm^3, monoclinic space group *C*2/*c*, *a* = 12.39880(10) Å, *b* = 17.17570(10) Å, *c* = 12.32030(10) Å, α = 90°, β = 92.7500(10)°, γ = 90°, *V* = 2620.69(3) Å^3, *Z* = 8, ρ_{calcd} = 1.840 g·cm^{-3}, μ = 11.827 mm^{-1}, *F*(000) = 1424, *T* = 100.00(10) K, R_1 = 0.0476, wR_2 = 0.1282, 2596 independent reflections [2θ ≤147.206°] and 172 parameters. CCDC 2180129 (**B**) contains the supplementary crystallographic data for this work. These data can be obtained free of charge via www.ccdc.cam.ac.uk/ data_request/cif (Cambridge Crystallographic Data Centre).

DFT/TDDFT calculations

Ground state geometry optimization of metal carbonyl complexes was carried out using Gaussian03,[3] with a Becke 3-parameter (exchange) Lee–Yang–Parr functional[4, 5] and LANL2DZ basis set. [6, 7] The local minimum structures of metal carbonyls were validated as minimum on the potential energy surface by computing vibrational modes. There were no phantom vibrations here. Time-dependent density functional theory calculations were done at CAM-B3LYP[8] /LANL2DZ level of theory, including the SMD solvation model.[9] Visualization of the electronic spectra and frontier molecular orbitals was achieved using Gaussview03.[10]

Myoglobin assay

By monitoring the conversion of Mb into Mb-CO species, the number of CO equivalents emitted by PhotoCORMs (**A** and **B**) was spectrophotometrically quantified by myoglobin assay.[11, 12] A buffered solution of standardised horse skeletal muscle myoglobin (Sigma-Aldrich) (0.1 M phosphate-buffered saline, pH = 7.4, 890 µL) was reduced in a quartz cuvette by adding 100 µL sodium dithionite solution. After that, 10 µL of CORMs in pure DMSO was added to complete the volume (1 mL) of the quartz cuvette. The stock solution concentrations were chosen to yield a final mixture of 10 µM dithionite, 60 µM myoglobin, and 10 µM CORM. 468 nm custom-built LED light source was used for illumination (Kingbright Elec. Co., 5000 mcd, part. no. BL0106-15-299). The photo flow of the light source (1.25×10^{-9} Einstein s^{-1}) was determined using the ferrioxalate actinometry test. The sealed cuvette was likewise positioned at a distance of 3 cm from the lamp, with the illumination interrupted at regular intervals to acquire UV/Vis spectra on Specord 210 Plus spectrophotometer until no more changes in the Q-band region were seen. Data was evaluated as described previously.[11, 12]

Biological activity

Materials and methods

Cell culture: The human triple negative breast cancer cell line (MDA-MB-231) and Human embryonic Kidney cells (HEK 283T) were obtained from VACSRA, Egypt, and maintained in Dulbecco's modified Eagle's medium (DMEM) and (RPMI 1640) respectively, supplemented with 4.5 g/L glucose, 4 mmol/L l-glutamine, 10% fetal bovine serum (FBS), and 10 U of penicillin and 10 mg L^{-1} of streptomycin as a monolayer culture at 37 °C in 5% CO_2 atmosphere. Cells were sub-cultured routinely to maintain the cells in a healthy condition.

Cell viability assay:

A. Evaluation of the cytotoxicity of PhotoCORMs (A and B)

The cytotoxicity of the two visible-induced PhotoCORMs (**A** and **B**) against MDA-MB-231 cells and HEK 293T was investigated using a 3-(4,5-dimethylthiazol-2-yl)-2,5-tetrazolium bromide (MTT) assay under both dark and illumination conditions. Cells were seeded into a 96-well plate at a density of 15,000 cells per well and incubated overnight. The rest of the MTT assay was performed in the dark to avoid the photo decomposition of compounds (**A** and **B**), unless otherwise mentioned. Cells were treated with different concentrations of the investigated complexes as follows: 0, 5, 10, 25 and 50 µM, and then incubated for 18 h to increase the uptake by the cells. After that, the media was removed, new media was added to the cells, and they were incubated for another 45 minutes. The cells were then exposed to light for 40

minutes at a distance of 3 cm. To test the effect of light, another plate was made under comparable conditions and then left in the dark as a control. The two plates were re-incubated for an additional 18 h. Afterward, media was removed, and cells were washed with PBS and MTT solution (0.5 mg ml^{-1}) was added on the cells. After 4 h of incubation, the MTT was replaced with 100 µL of DMSO to dissolve the generated formazan crystals. After shaking the plates for 15–20 min, the absorbance was recorded using a Wallac 1420 Victor2 Multilabel Counter (Perkin Elmer Inc., Waltham, MA, USA) at 490 nm. The relative cell viability was determined by normalizing the absorbance of the treated cells to untreated cells. The inhibitory concentration (IC_{50}), at which 50% of the cells are killed was determined by non-regression analysis of the dose–response curve using Graph Pad Prism software.

B. Evaluation of the cytotoxicity of complex B in combination with Paclitaxel

The cytotoxicity of the synthesized tricarbonyl Mn(I) complexes, with and without illumination, against MDA-MB-231 cells was investigated using a 3-(4,5-dimethylthiazol-2-yl)-2,5-tetrazolium bromide (MTT) assay. Cells were seeded into a 96-well plate at a density of 15000 cells per well and incubated overnight. The rest of the MTT assay was performed in the dark, unless otherwise mentioned. Cells were treated with the chemotherapeutic agent alone (Paclitaxel) according to the following concentrations (0, 1, 3, 10, and 30 nM) or treated with complex **B** alone according to the following concentrations (0, 5, 10, 25 and 50 µM) or co-treated with both the complex **B** at different concentrations with the highest concentration of Paclitaxel (30 nM) and then incubated for 48 h to increase the uptake by the cells. After that, media were removed, and fresh media were added to the cells and then they were incubated again for 45 min. Next, the cells were exposed to light at a distance of 3 cm for 40 min. Another plate was prepared under similar conditions and then kept in the dark as a control to investigate the effects of light. The two plates were re-incubated for an additional 18 h. Afterward, media was removed, and cells were washed with PBS and MTT solution (0.5 mg ml^{-1}) was added on the cells. After 4 h of incubation, the MTT was replaced with 100 µL of DMSO to dissolve the formed formazan crystals. After shaking the plates for 15–20 min, the absorbance was recorded using a Wallac 1420 Victor2 Multilabel Counter (Perkin Elmer Inc., Waltham, MA, USA) at 490 nm. The relative cell viability was determined by normalizing the absorbance of the treated cells to untreated cells.

Statistical Analysis

All experiments were performed in triplicates and repeated at least three times. All data are presented as the mean ± standard error of the mean. All analyses were performed using GraphPad Prism Software. $P<0.05$ was considered statistically significant with One-way ANOVA test. ***=$p<0.001$, **=$p<0.01$, *=$p<0.05$

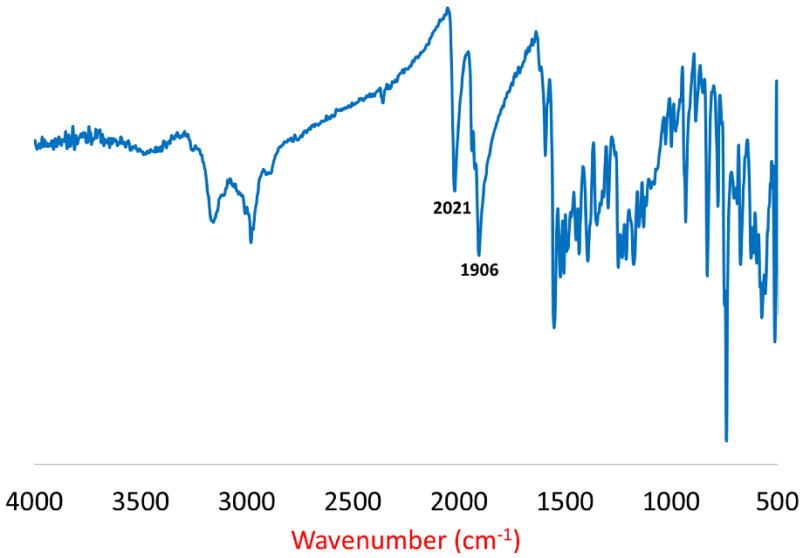

a)

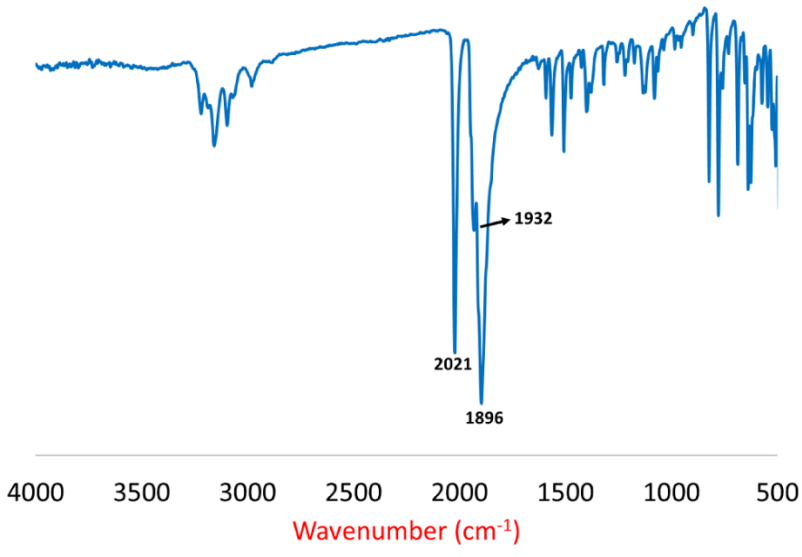

b)

Fig. S1 IR spectra of *fac*-[MnBr(CO)$_3$L] complexes, a) L **=** quinoline-2-carboxaldehyde (**A**) and b) L = 8-amino quinoline (**B**)).

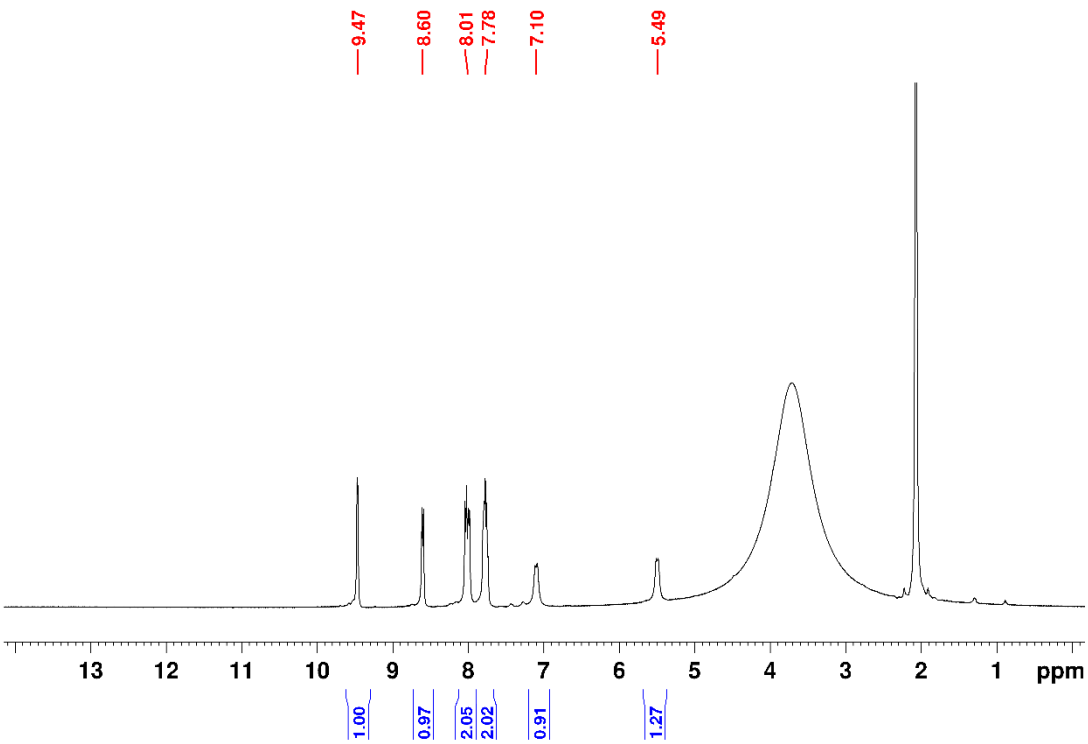

Fig. S2 ^{1}H NMR spectrum (in CD_3COCD_3) of complex **B**.

Table S1 Single-crystal X-ray diffraction data of complex **B**.

Data	**B**
Empirical formula	$C_{12}H_8BrMnN_2O_3$
Formula weight ($g \cdot mol^{-1}$)	363.05
Temperature (K)	100.00(10)
Radiation, λ (Å)	$Cu_{K\alpha}$, 1.54184
Crystal system	orthorhombic
Space group	*Pbca*
Unit cell dimensions	
a (Å)	17.7147(2)
b (Å)	12.0111(2)
c (Å)	25.1224(3)
α (°)	90
β (°)	90
γ (°)	90
Volume ($Å^3$)	5345.37(13)
Z	16
Calculated density ($Mg \cdot m^{-3}$)	1.805
Absorption coefficient (mm^{-1})	11.596
F(000)	2848
Theta range for collection	3.519 to 73.763°
Reflections collected	30471
Independent reflections	5342
Minimum/maximum transmission	0.195/0.753
Refinement method	Full-matrix least-squares on F^2
Data / parameters / restraints	5342 / 343 / 0
Goodness-of-fit on F^2	1.101
Final R indices [I>2σ(I)]	R_1 = 0.0277, wR_2 = 0.0691
R indices (all data)	R_1 = 0.0327, wR_2 = 0.0709
Maximum/minimum residual electron density ($e \cdot Å^{-3}$)	0.716 / –0.523

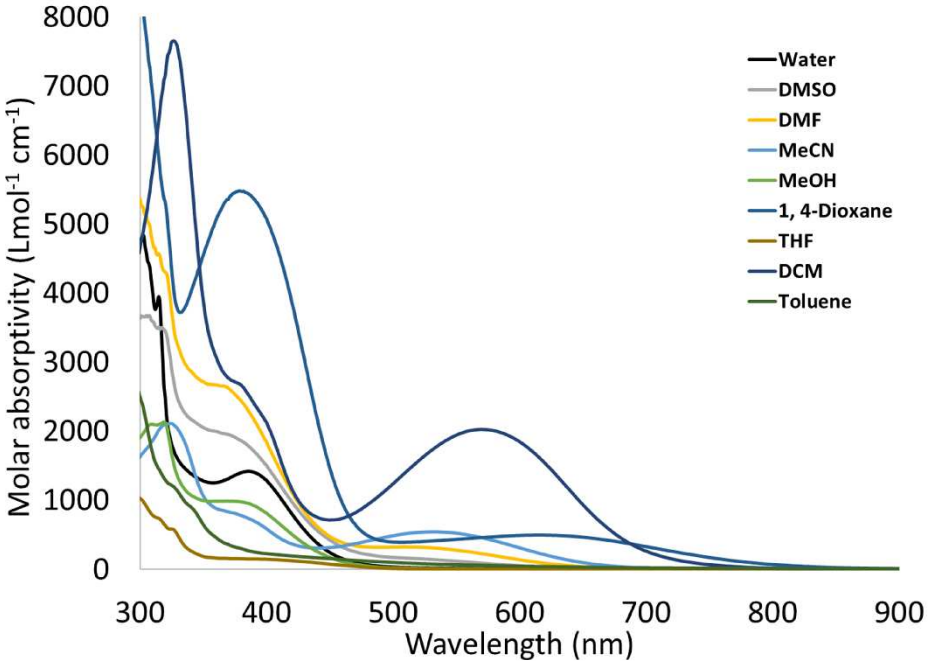

Fig. S3 Electronic absorption spectra of complex **A** in different solvents.

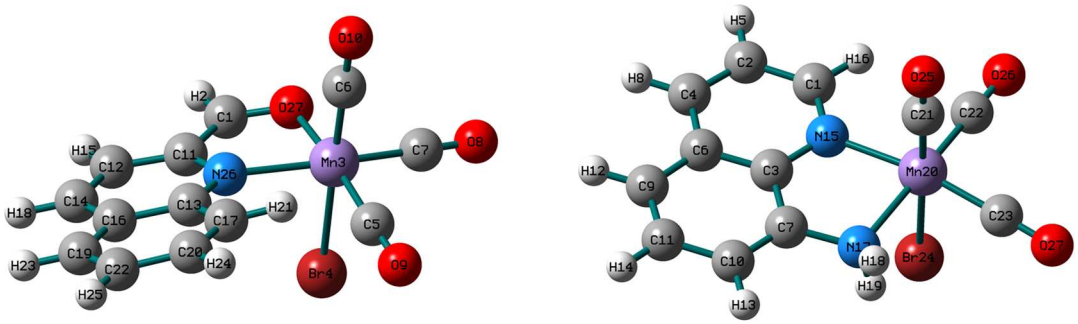

a) **b)**

Fig. S4 The local minimum structures of a) **A** and b) **B**.

Table S2 Selected experimental bond lengths (Å) and angles (°) of complexes **A** and **B**.

	A	**B**
Mn–C1	1.802	1.793
Mn–C2	1.815	1.809
Mn–C3	1.827	1.818
Mn–N1	_____	2.109
Mn–O	2.0198	_____
Mn–N10	2.103	2.053
Mn–Br	2.584	2.614
C1–O1	1.181	1.184
C2–O2	1.178	1.179
C3–O3	1.173	1.178
C1–Mn–C2	94.19	93.9
C1–Mn–C3	93.39	93.5
C1–Mn–N1	_____	94.8
C1–Mn–O	95.6	_____
C1–Mn–N10	_____	92.0
C1–Mn–Br	177.8	177.9
C2–Mn–C3	89.9	90.8
N1–Mn–C2	_____	170.4
O–Mn–C2	170.1	_____
C2–Mn–N10	101.5	95.3
C2–Mn–Br	83.6	88.0
N1–Mn–C3	_____	92.3
O–Mn–C3	88.3	_____
C3–Mn–N10	165.59	171.3
C3–Mn–Br	86.58	86.6
N1–Mn–N10	_____	80.5
N10–Mn–O	78.9	_____
N1–Mn–Br	_____	83.1
O–Mn–Br	86.57	_____
N10–Mn–Br	86.0	87.53

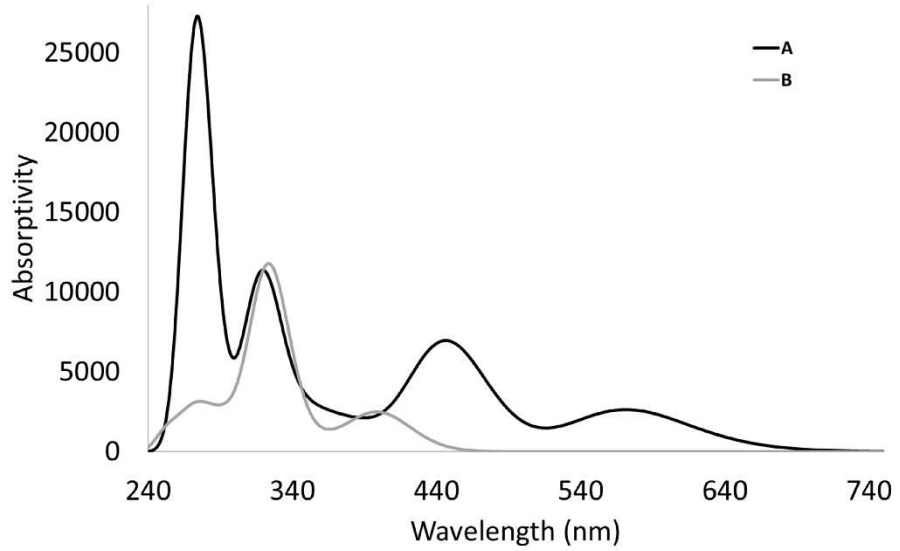

a)

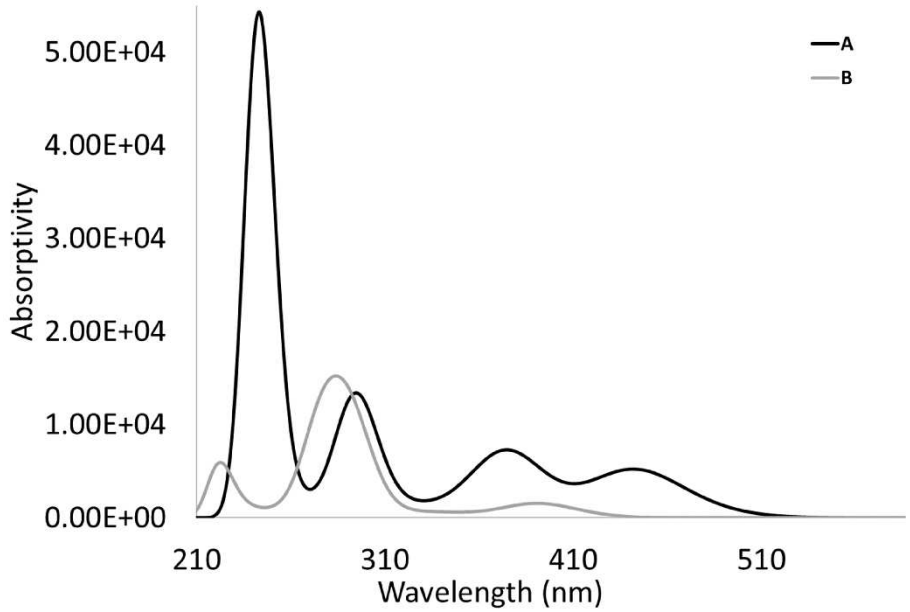

b)

Fig. S5 TD-DFT calculated spectra of complexes **A** and **B**, calculated at **a)** B3LYP/LANL2DZ and **b)** CAM-B3LYP/LANL2DZ level of theories.

Table S3 Computed excitation energies (eV), electronic transition configurations and oscillator strengths (*f*) of compounds **A** and **B** (selected, $f > 0.001$)			
Energy (cm^{-1})	Wavelength (nm)	*f*	Major contributions
• **A (B3YLP/LANL2DZ)**			
15685	637	0.0006	HOMO→LUMO (97%)
17501	571	0.036	HOMO–1→LUMO (98%)
20105	497	0.0004	HOMO–3→LUMO (80%)
21928	456	0.0501	HOMO–2→LUMO (69%)
22853	437	0.0519	HOMO–4→LUMO (86%)
28319	353	0.0262	HOMO–6→LUMO (84%)
25817	387	0.0102	HOMO–5→LUMO (80%)
31179	320	0.0916	HOMO–7→LUMO (55%)
36433	274	0.1797	HOMO–2→LUMO+1 (29%)
• **A (CAM-B3YLP/LANL2DZ)**			
21056	474	0.0026	HOMO→LUMO (86%)
22615	442	0.0696	HOMO–1→LUMO (90%)
24957	400	0.0005	HOMO–3→LUMO (56%)
25142	397	0.0026	HOMO–3→LUMO (21%)
26603	375	0.0619	HOMO–2→LUMO (54%)
26873	372	0.0198	HOMO–3→LUMO+14 (21%), HOMO–2→LUMO (23%)
28360	352	0.0171	HOMO–4→LUMO (79%)
30387	329	0.0039	HOMO–3→LUMO+2 (28%)
31417	318	0.0069	H–5→LUMO (69%)
33826	295	0.1388	HOMO–7→LUMO (43%), HOMO–6→LUMO (33%)
40212	248	0.0711	HOMO→LUMO+1 (68%)
40838	244	0.113	HOMO–1→LUMO+1 (27%)
41639	240	0.3295	HOMO–10→LUMO (23%)
• **B (B3YLP/LANL2DZ)**			
247372	404	0.0214	HOMO→LUMO (45%), HOMO→LUMO+1 (26%)
25254	395	0.0101	HOMO–1→LUMO (35%), HOMO–1→LUMO+1 (29%)
26703	374	0.0076	HOMO→LUMO (47%)
27630	361	0.0021	HOMO–1→LUMO (32%)
28027	356	0.0001	HOMO–1→LUMO (28%)
29608	337	0.0042	HOMO–3→LUMO (29%)
30874	323	0.1228	HOMO–2→LUMO (67%)
32748	305	0.0028	HOMO–4→LUMO (46%)
34107	293	0.0133	HOMO–5→LUMO (75%)
37197	268	0.009	HOMO–6→LUMO (83%)
• **B (CAM-B3YLP/LANL2DZ)**			
25280	395	0.0065	HOMO→LUMO+2 (28%)
25684	389	0.0148	HOMO–1→LUMO+2 (26%)
28099	355	0.0021	HOMO–3→LUMO+2 (40%)
28849	346	0.0037	HOMO–3→LUMO+3 (36%)
30945	323	0.0032	HOMO–1→LUMO+3 (22%)

32824	304	0.001	HOMO–4→LUMO+4 (27%), HOMO–1→LUMO+4 (22%), HOMO→LUMO+4 (25%)
33848	295	0.0174	HOMO–3→LUMO +4 (21%), HOMO→LUMO (23%)
34185	292	0.1067	HOMO→LUMO (58%)
35667	280	0.0475	HOMO–2→LUMO (33%), HOMO–1→LUMO (45%)
35983	277	0.0777	HOMO–2→LUMO (47%), HOMO–1→LUMO (34%)
45359	220	0.0438	HOMO→LUMO+1 (22%)

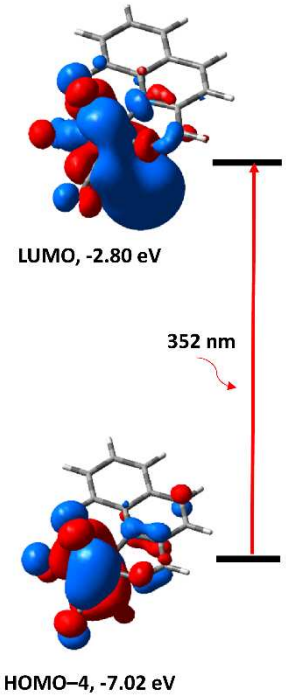

Fig. S6 The electronic transition at 352 nm and frontier molecular orbitals of complex **A** calculated at CAM-B3LYP/LANL2DZ level of theory.

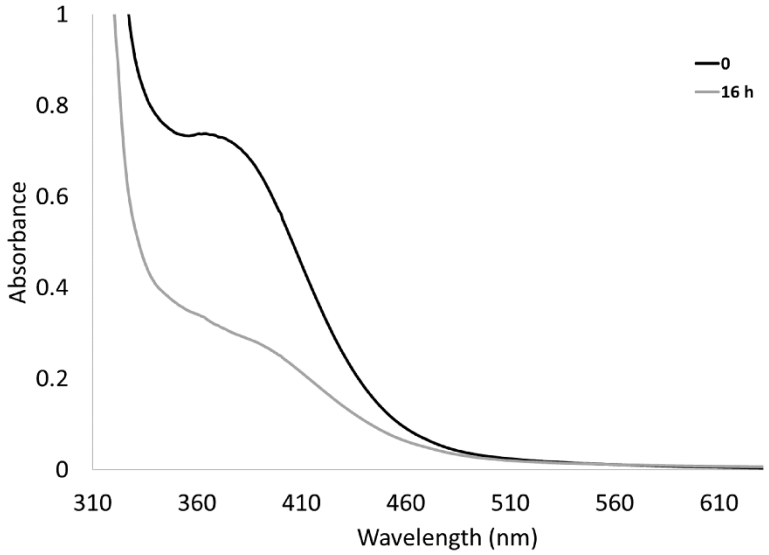

a)

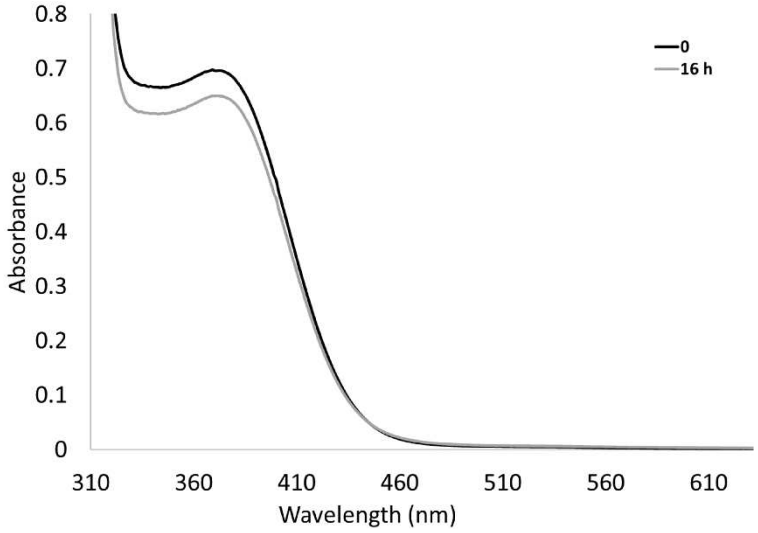

b)

Fig. S7 Electronic absorption changes upon incubation of complexes a) **A** (0.25 mM) and b) **B** (0.24 mM) in DMSO/H_2O mixture in the dark for 16 h.

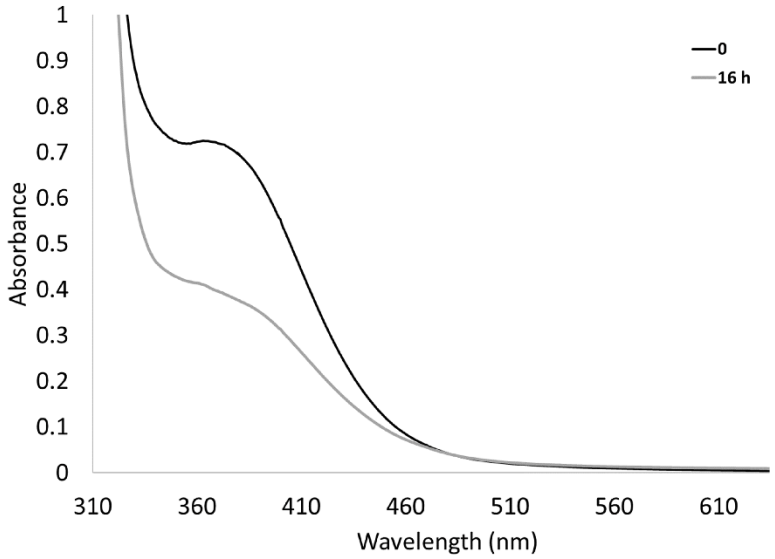

a)

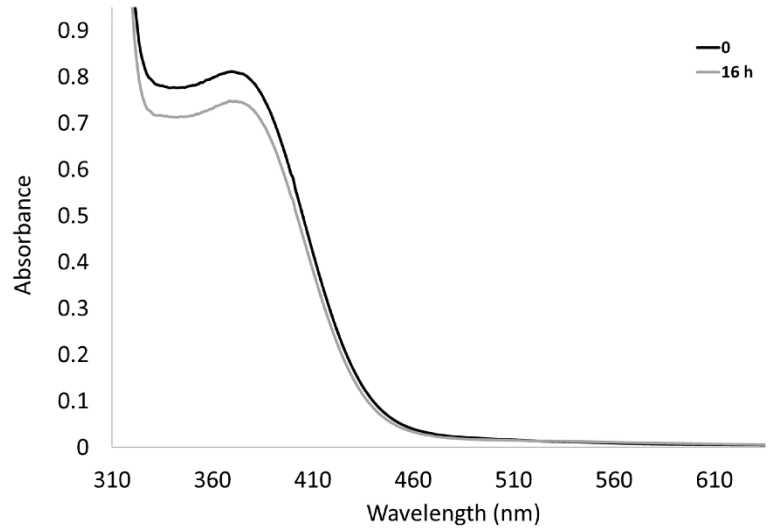

b)

Fig. S8 Electronic absorption changes upon incubation of complexes a) **A** (0.25 mM) and b) **B** (0.24 mM) in an excess of sodium bromide in the dark for 16 h.

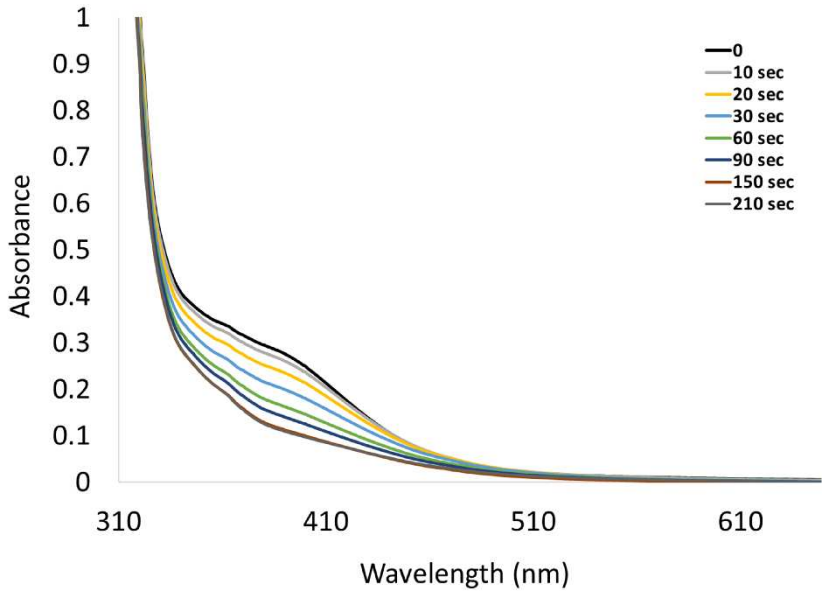

Fig. S9 UV/Vis spectral changes of complex **A** (0.25 mM in DMSO-H_2O mixture) upon photolysis at 468 nm with increasing illumination time (0–210 seconds).

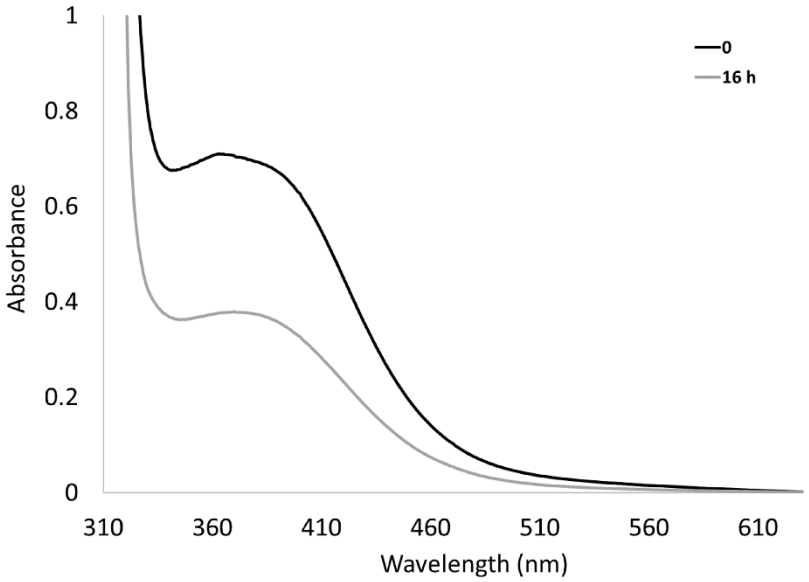

a)

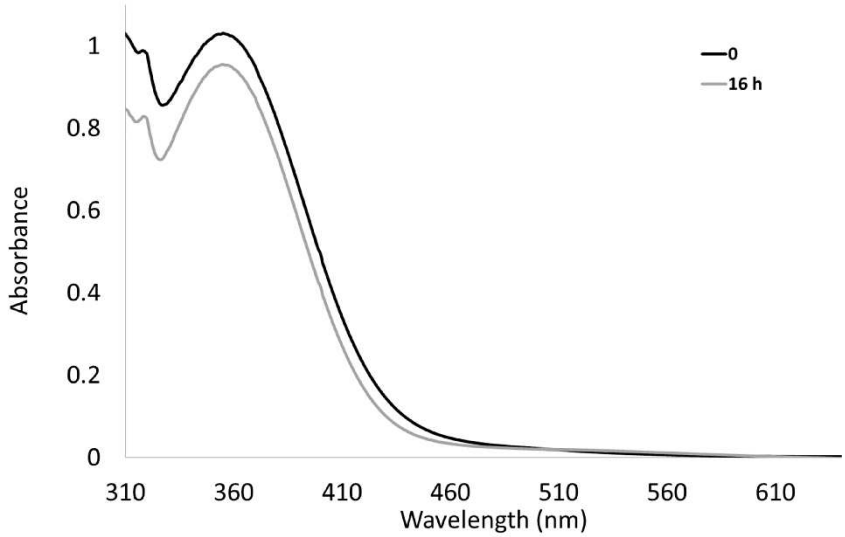

b)

Fig. S10 Electronic absorption changes upon incubation of complexes a) **A** (0.25 mM) and b) **B** (0.24 mM) in sodium dithionite in the dark for 16 h.

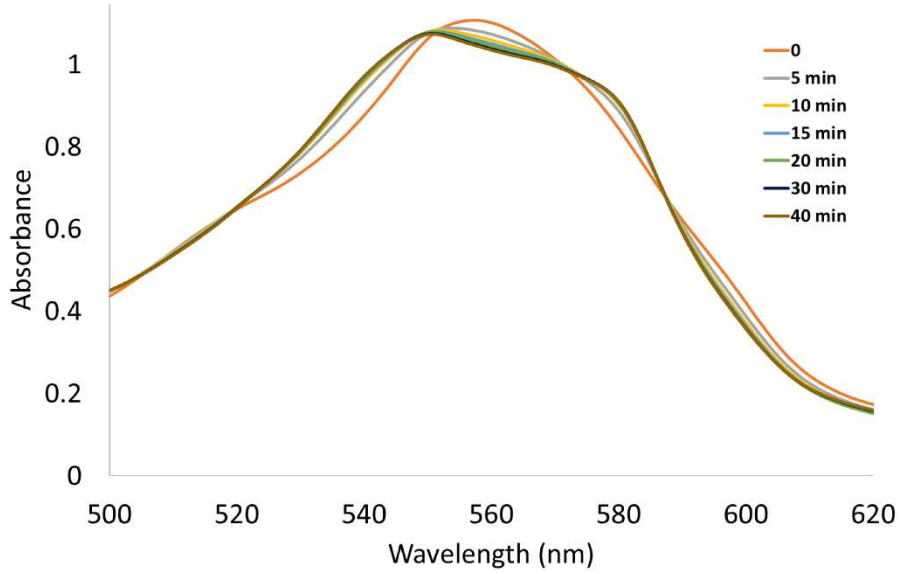

Fig. S11 UV/vis spectral changes in the Q-band region of myoglobin (60 µM in 0.1 PBS at pH 7.4) with sodium dithionite (10 mM) and complex **A** (10 µM) under a dinitrogen atmosphere upon photolysis at 468 nm.

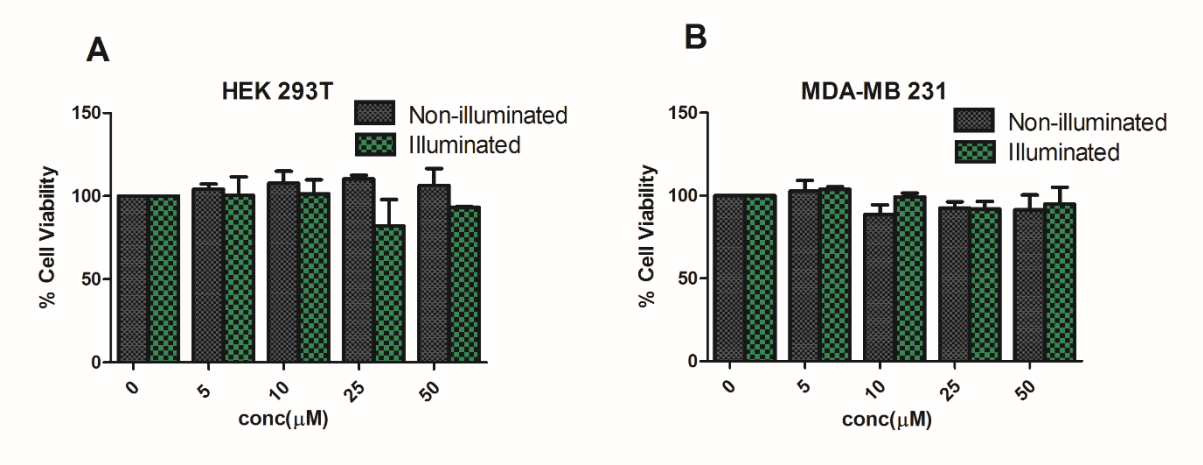

Fig. S12 Comparison of cell viability of HEK 293T and MDA-MB-231 treated with different concentrations of compound **A** under both dark and illumination conditions.

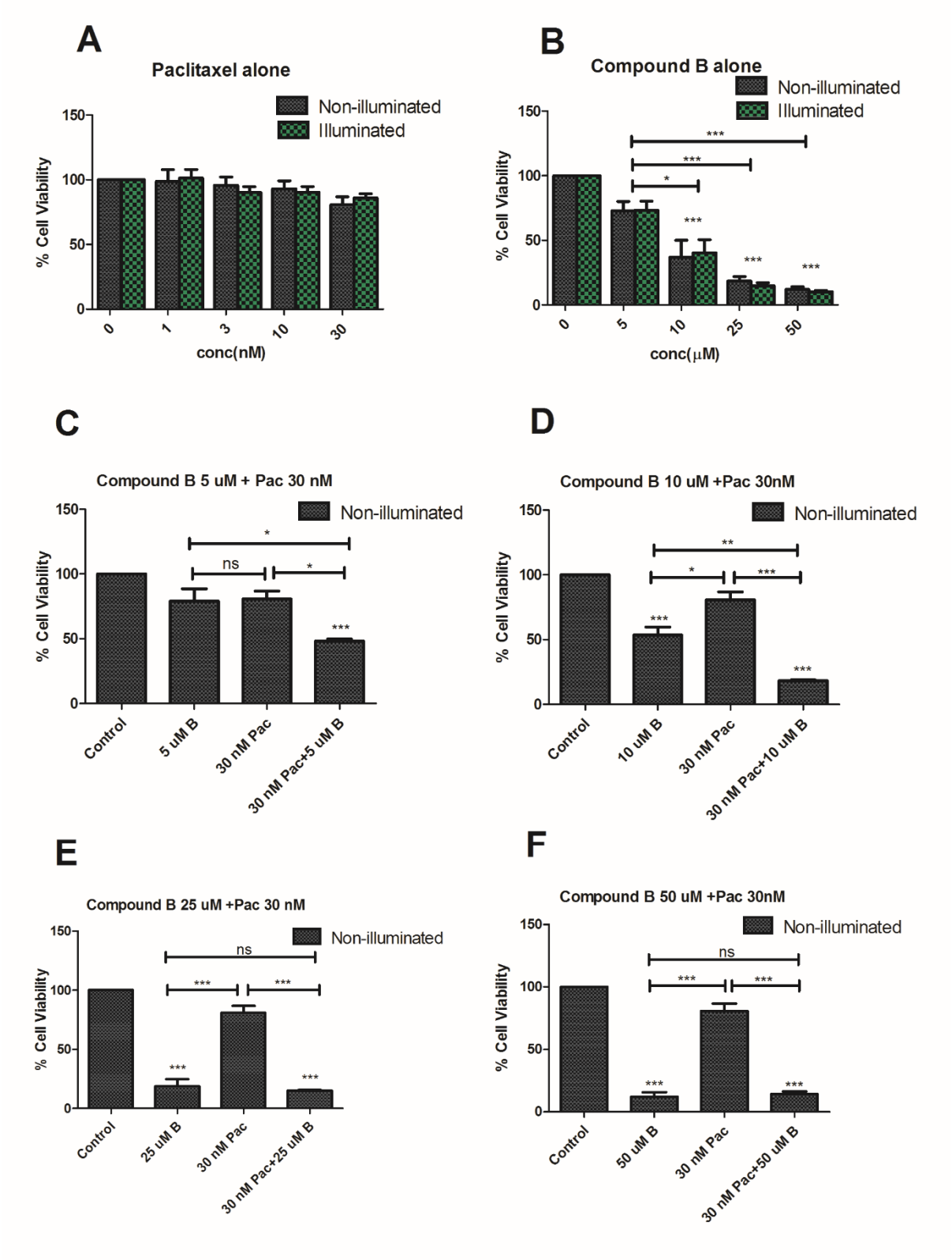

Fig. S13 Comparison of cell viability of MDA-MB-231 treated with (A) paclitaxel alone, and (B) compound **B** alone**,** in different concentrations. (C, D, E, F) co-treatment of MDA-MB-231 cells with paclitaxel (30 nM) and compound **B** in different concentrations (5 μM, 10 μM, 25 μM and 50 μM) respectively, under dark conditions. Asterisks on the bar itself show results of

statistically significant difference when compared to control group, while the ones indicated by line with asterisks show statistically significant difference compared to different groups as indicated. P<0.05 was considered statistically significant with One-way ANOVA test. ***=p<0.001, **=p<0.01, *=p<0.05

References

1. G. M. Sheldrick, SHELXT–Integrated space-group and crystal-structure determination, *Acta Crystallogr., Sect. A: Found. Adv.*, 2015, **71**, 3-8.
2. G. M. Sheldrick, A short history of SHELX, *Acta Crystallogr., Sect. A: Found. Crystallogr.*, 2008, **64**, 112-122.
3. M. J. Frisch, G. W. Trucks, H. B. Schlegel, G. E. Scuseria, M. A. Robb, J. R. Cheeseman, V. G. Zakrzewski, J. A. Montgomery, J. C. B. R. E. Stratmann, S. Dapprich, J. M. Millam, A. D. Daniels, K. N. Kudin, M. C. Strain, O. Farkas, J. Tomasi, V. Barone, M. Cossi, R. Cammi, B. Mennucci, C. Pomelli, C. Adamo, S. Clifford, J. Ochterski, G. A. Petersson, P. Y. Ayala, Q. Cui, K. Morokuma, D. K. Malick, A. D. Rabuck, K. Raghavachari, J. B. Foresman, J. Cioslowski, J. V. Ortiz, A. G. Baboul, B. B. Stefanov, A. L. G. Liu, I. K. P. Piskorz, R. Gomperts, R. L. Martin, D. J. Fox, T. Keith, M. A. Al-Laham, C. Y. Peng, A. Nanayakkara, C. Gonzalez, M. Challacombe, P. M. W. Gill, B. G. Johnson, W. Chen, M. W. Wong, J. L. Andres, M. Head-Gordon, E. S. Replogle and J. A. Pople, *GAUSSIAN 03 (Revision A.9), Gaussian, Inc., Pittsburgh*, 2003.
4. A. Becke, Density-functional thermochemistry. III. The role of exact exchange (1993) J, *Chem. Phys*, **98**, 5648.
5. A. D. Becke, Density-functional exchange-energy approximation with correct asymptotic behavior, *Phys. Rev. A*, 1988, **38**, 3098.
6. P. J. Hay and W. R. Wadt, Ab initio effective core potentials for molecular calculations. Potentials for K to Au including the outermost core orbitals, *J. Chem. Phys.*, 1985, **82**, 299-310.
7. P. J. Hay and W. R. Wadt, Ab initio effective core potentials for molecular calculations. Potentials for the transition metal atoms Sc to Hg, *J. Chem. Phys.*, 1985, **82**, 270-283.
8. T. Yanai, D. P. Tew and N. C. Handy, A new hybrid exchange–correlation functional using the Coulomb-attenuating method (CAM-B3LYP), *Chem. Phys. Lett.*, 2004, **393**, 51-57.
9. A. V. Marenich, C. J. Cramer and D. G. Truhlar, Universal solvation model based on solute electron density and on a continuum model of the solvent defined by the bulk dielectric constant and atomic surface tensions, *J. Phys. Chem. B*, 2009, **113**, 6378-6396.
10. A. Frisch, A. B. Nielson and A. J. Holder, Gaussview User Manual, *Gaussian, Inc., Pittsburgh, PA*, 2000, .
11. S. McLean, B. E. Mann and R. K. Poole, Sulfite species enhance carbon monoxide release from CO-releasing molecules: implications for the deoxymyoglobin assay of activity, *Analytical biochemistry*, 2012, **427**, 36-40.
12. A. J. Atkin, J. M. Lynam, B. E. Moulton, P. Sawle, R. Motterlini, N. M. Boyle, M. T. Pryce and I. J. Fairlamb, Modification of the deoxy-myoglobin/carbonmonoxy-myoglobin UV-vis assay for reliable determination of CO-release rates from organometallic carbonyl complexes, *Dalton Trans.*, 2011, **40**, 5755-5761.